IEEE Access
Multidisciplinary | Rapid Review | Open Access Journal

Received October 2, 2021, accepted October 8, 2021, date of publication October 13, 2021, date of current version October 21, 2021.

Digital Object Identifier 10.1109/ACCESS.2021.3119625

Development of Optimized Cooperative Control Based on Feedback Linearization and Error Port-Controlled Hamiltonian for Permanent Magnet Synchronous Motor

YUJIAO ZHAO[1], HAISHENG YU[1], AND SHIXIAN WANG[2]
[1]Shandong Key Laboratory of Industrial Control Technology, College of Automation, Qingdao University, Qingdao 266071, China
[2]School of Mechanical, Electrical and Information Engineering, Shandong University at Weihai, Weihai 264209, China

Corresponding author: Haisheng Yu (yu.hs@163.com)

This work was supported in part by the National Natural Science Foundation of China under Grant 61573203.

ABSTRACT The conflict between dynamic rapidity and steady-state accuracy is a crucial factor hindering the performance improvement of motor control system. To overcome the issue, this article proposes an optimized cooperative control combining feedback linearization (FBL) and error port-controlled Hamiltonian (EPCH) for permanent magnet synchronous motor (PMSM). First, FBL and EPCH are separately designed to obtain good dynamic and steady-state performances. Then, considering the individual advantages of FBL and EPCH, a cooperative strategy based on the real-time position error is applied to realize the smooth switching between the two methods, so that each method is utilized efficiently within the corresponding operating range. In addition, the particle swarm optimization (PSO) algorithm is introduced to properly select the controller parameters. Thus, an optimized cooperative control method, which takes into account both fast dynamic response and high steady-state precision, is developed for PMSM drives. The experimental results are finally given to illustrate the effectiveness and superiority of the proposed method.

INDEX TERMS Permanent magnet synchronous motor, cooperative control, parameter optimization.

I. INTRODUCTION

Due to the inherent characteristics of simple structure, good reliability and high energy efficiency, permanent magnet synchronous motor (PMSM) drive system and its control are known as an attractive research topic in the industrial applications, such as electric vehicles, robots, machine tools [1]. Precise and fast tracking performances are of high demand in many of these applications [2]– [4]. However, as the individual control method could not provide a satisfactory response, many hybrid control strategies have been developed for PMSM drive system in recent years. Besides, the selection of the controller parameters, as a key factor to reach the desired response, has motivated the scientists to investigate the optimization issue [5].

Many solutions have been discussed from the aspects of rapidity, stability and accuracy to realize the high-performance tracking of the PMSM drive system. These control methods are usually categorized into two types. One is represented by the method based on the signal transformation, such as predictive control, sliding mode control, fuzzy control, and feedback linearization control. The feedback linearization (FBL) control method converts the complex nonlinear system into an equivalent linear system through state feedback and coordinate transformation, so that the dynamic response time can be adjusted by assigning poles. Due to its advantages of fast dynamic response, FBL control method has received deep investigation in recent research works [6]–[10]. Liu *et al.* have shown the effectiveness of this method for the PMSM drive system [8]. Meng *et al.* have applied an input/output feedback linearization controller to deal with the nonlinear and coupling characteristics of a quadruple-tank liquid level system [9]. In [10], only one controller for all state space variables has been designed. In [11], a state feedback controller based on gray wolf optimization algorithm has been designed for the high performance

The associate editor coordinating the review of this manuscript and approving it for publication was Alfeu J. Sguarezi Filho.

control of a permanent-magnet synchronous hub motor (PMSHM) drive, in which the linearized PMSHM mathematical model is obtained by voltage feedforward compensation. A similar problem also appears in [12], Sun *et al.* have applied the state feedback control to solve the coupling and nonlinear of bearingless permanent magnet synchronous machine. However, in practical applications, the FBL method has fluctuation in steady-state operation, which seriously reducing the trajectory tracking accuracy. The other is based on the energy transformation control strategy. The port-controlled Hamiltonian (PCH) method based on interconnection and damping assignment is a popular approach for nonlinear systems because of its simple model structure, convenient stability analysis and excellent steady-state characteristics [13], [14]. This method has been well applied in industry [15]–[17]. However, the PCH method is not flawless; indeed, the slow response problem to disturbances hinders the wide application of this method. Obviously, these approaches can only improve the control performance in specific aspects, not overall. This means that none of them is an effective solution for good position tracking.

In order to break these limitations, the combination of different methods is considered to be a suitable scheme. For instance, in [18], an optimal FBL control has been presented for PMSM to achieve accurate tracking and energy saving by minimizing the copper loss. Campos-Rodriguez *et al.* have proposed a hybrid cascade control considering the trade-off between safety, productivity and quality for the nonlinear dynamical system. This structure includes two robust nonlinear regulators, a discrete regulator for the outer loop and a continuous regulator for the inner loop [19]. Song *et al.* have implemented an improved model predictive control (MPC) to simultaneously consider both system efficiency and identification accuracy to determine the optimal power distribution between super-capacitor and battery [20]. Jiang *et al.* have presented an improved deadbeat predictive control (DBPC) method based sliding mode control (SMC) to improve the driving performance of PMSM, in which SMC and DBPC are applied to control speed and current, respectively [21]. Although these methods can be conducive to the improvement of motor performance, they are actually based on a cascade control structure, which means a compromise between dynamic rapidity and steady-state accuracy. High steady-state precision should not be at the expense of dynamic response [22]. How to simultaneously achieve fast dynamic response and good steady-state accuracy is the emphases and difficulties in the field of control engineering.

The reasonable application of the control methods under different operation conditions is another solution. The concept of cooperative control is thus proposed [23]–[25]. Its basic working principle is to design a control strategy to realize the switching control between different methods, so that each method can be effectively used in the corresponding working range. In [26], the pump drives the actuator in an efficient way and the valves are controlled to provide the tracking accuracy, thus the pump–valve-coordinated system could achieve the dual goals of high control performance and high energy efficiency. Wang *et al.* have designed a compound torque regulator which combines two new variable hysteresis bands and two constant hysteresis bands to optimize the torque tracking performance of PMSM drives [27]. This method can improve the steady-state and dynamic torque tracking performances while maintaining the advantages of the conventional direct torque control. Hao *et al.* have integrated the merits of linear active disturbance rejection control (ADRC) and nonlinear ADRC, and overcame their shortcomings by a hysteretic switching strategy to achieve good robustness and precision for PMSM [28]. In [29], a hybrid speed control composed of parallel connected SMC and neuro fuzzy control (NFC) has been introduced for PMSM drives. Using the bandwidth error, the control system can get satisfactory dynamic response both in transient and steady-state modes. In [30], a cooperative control method based on DBPC and PCH has been applied to achieve high performance and high efficiency for PMSM. In this way, the overall performance of the PMSM drive system is improved. However, the DBPC controller only shortens the dynamic response time of the current loop. Thus, to indeed guarantee the control performance of PMSM drive system, new control method based on cooperative control theory is urgent to be further developed.

In addition, the parameter tuning plays an important role in the realization of the control objectives and the optimization of the controllers. The previous experience has certain guiding significance for selecting the initial values of the controller parameters. However, without the sufficient information of the controlled system, the selection of the appropriate controller parameters could be a tedious trial and error process. To this end, computer-aided optimization algorithms have been suggested to find the best possible coefficients of controllers in some literature. In [31], an adaptive ant colony algorithm has been applied in the path planning optimization of a robot system. Mahmoudabadi *et al.* have utilized an improved particle swarm optimization (PSO) algorithm to optimize the decoupling sliding-mode control of a ball and beam system [32]. In [33], a genetic algorithm has been employed to optimize the design of a multi-input active disturbance rejection controller. In [34], a simulated annealing method has been introduced to solve the motor efficiency optimization problem of electric vehicles.

In this article, motivated by the above discussions, an optimized cooperative control strategy based on the signal controller and the energy controller is proposed to improve the dynamic and steady state performances of the PMSM drive system simultaneously. The signal controller is designed by using FBL control method to provide a fast dynamic response, and the energy controller is developed using EPCH control method to obtain a good steady-state response. The cooperative control strategy is implemented by using the convex combination based on the position error, so as to regulate the output strength of the signal controller and the energy

controller. The observer is presented to estimate unknown load torque. Furthermore, PSO algorithm is applied to properly select the control gains. The cost function of the optimization process is defined as the integral of time multiplied by absolute error and is minimized. The experimental results show that the proposed control method has good dynamic and steady-state performances.

The main innovations and contributions of the control method proposed in this article are as follows:

1) The cooperative control strategy is designed so that the PMSM drive system can combine simultaneously the advantages of both signal control and energy control and obtain the smooth output response without control signal shaking.
2) The cooperative control system is constructed. Through theoretical analysis and experimental verification, it is proved that the system not only exhibits fast tracking control of position signal, but also optimizes the input and output energy of the PMSM drive system.
3) A novel perspective on the overall performance improvement of the PMSM system is created by focusing on the reasonable distribution of the control methods. Meaningfully, such control method can be extended to other nonlinear systems as a good candidate for high trajectory tracking applications.

The rest of this article is organized as follows. In Section II, the mathematical model of a PMSM drive system is described. In Section III, the design process of FBL controller, EPCH controller and load torque observer is given. In Section IV, the cooperative control strategy is presented with a detailed proof. Additionally, the PSO algorithm is introduced to adjust the control gains. In Section V, the experimental results are presented to validate the effectiveness by comparing with other existing control methods. Section VI concludes this article.

II. MATHEMATICAL MODEL OF PMSM

The mathmetical model of the non-salient PMSM in the synchronous reference frame is expressed as [3]:

$$\begin{cases} L\dfrac{di_d}{dt} = -R_s i_d + n_p \omega L i_q + u_d \\ L\dfrac{di_q}{dt} = -R_s i_q - n_p \omega L i_d - n_p \omega \Phi + u_q \\ J_m\dfrac{d\omega}{dt} = \tau - \tau_L - R_f \omega = n_p \Phi i_q - \tau_L - R_f \omega \\ \dfrac{d\theta}{dt} = \omega \end{cases} \tag{1}$$

where i_d and i_q are the stator currents in the d-q axis, u_d and u_q are the stator voltages in the d-q axis, τ and τ_L are the electromagnetic torque and load torque, respectively. ω is the mechanical angular of the motor, θ is the angle of the motor, R_s is the stator resistance, L is the stator inductance, Φ is the permanent magnet flux. J_m is the moment of inertia, n_p is the number of the pole pairs. R_f is the viscous friction coefficient.

The control objective is to find a controller which can ensure the internal stability and adjust the stator voltage to track the position reference. Meanwhile, the control system can obtain fast dynamic response and high steady-state accuracy. This problem will be solved in two steps. Fig.1 shows the general PMSM drive system structure.

III. DESIGN OF INDIVIDUAL CONTROLLERS

A. DESIGN OF LOAD TORQUE OBSERVER

In order to improve the robustness of the closed-loop control system, a Luenberger observer is first designed to track load disturbance in real time, and the estimated disturbance is considered as the feedforward to compensate the voltage reference. The load torque observer is constructed as follows [17]:

$$\begin{cases} \dot{\hat{\theta}} = \hat{\omega} + l_1\left(\theta - \hat{\theta}\right) \\ \dot{\hat{\omega}} = \dfrac{n_p \Phi i_q - \hat{\tau}_L - R_f \hat{\omega}}{J} + l_2\left(\theta - \hat{\theta}\right) \\ \dot{\hat{\tau}}_L = l_3\left(\theta - \hat{\theta}\right) \end{cases} \tag{2}$$

where $\hat{\theta}$, $\hat{\omega}$ and $\hat{\tau}_L$ are position estimation, speed estimation and load torque estimation respectively. By choosing the appropriate gains l_1, l_2 and l_3, the estimation error can be exponentially reduced to zero.

B. DESIGN OF FBL

PMSM can be considered as a nonlinear system and expressed by the following equation:

$$\dot{x}_f = f(x) + g_1(x)\, u_{fd} + g_2(x)\, u_{fq} \tag{3}$$

where

$$\begin{aligned} x_f &= \left[\, x_{f1}\ x_{f2}\ x_{f3}\ x_{f4} \,\right]^T = \left[\, i_d\ i_q\ \omega\ \theta \,\right]^T \\ g_1(x) &= \left[\, \tfrac{1}{L}\ 0\ 0\ 0 \,\right]^T \\ g_2(x) &= \left[\, 0\ \tfrac{1}{L}\ 0\ 0 \,\right]^T \\ f(x) &= \begin{bmatrix} -\dfrac{R_s}{L} i_d + n_p \omega i_q \\ -\dfrac{R_s}{L} i_q - n_p \omega i_d - \dfrac{1}{L} n_p \omega \Phi \\ \dfrac{1}{J_m} n_p i_q \Phi - \dfrac{1}{J_m} R_f \omega - \dfrac{1}{J_m} \hat{\tau}_L \\ \omega \end{bmatrix} \end{aligned}$$

It can be seen that the motor model (3) contains nonlinear and cross-coupled terms in the first and second rows of the state space equation.

First, choose the output variable as:

$$y_f = \left[\, y_{f1}\ y_{f2} \,\right]^T = \left[\, i_d\ \theta \,\right]^T \tag{4}$$

According to feedback linearization control theory, the output variables are differentiated repeatedly until the relationship between the input variable and the time is found, which

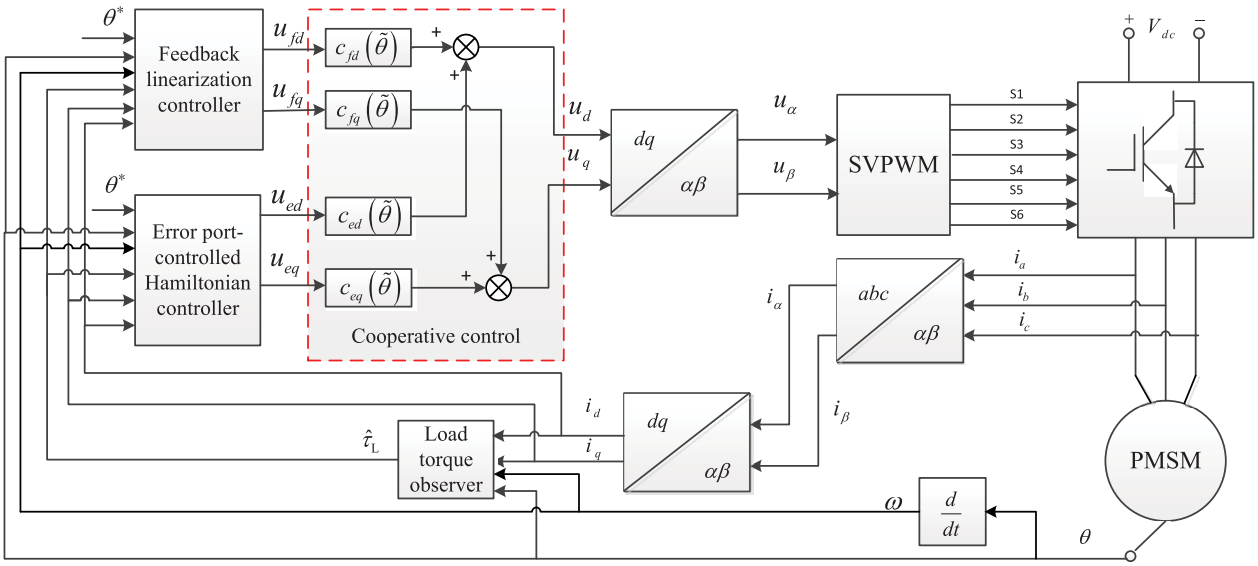

FIGURE 1. Block diagram of PMSM drive system with optimized cooperative control.

could be represented as follows:

$$\begin{cases} \dfrac{dy_{f1}}{dt} = -\dfrac{R_s}{L} i_d + n_p \omega i_q + \dfrac{1}{L} u_{fd} \\ \dfrac{dy_{f2}}{dt} = \omega \\ \dfrac{d^2 y_{f2}}{dt^2} = \dfrac{1}{J_m} n_p i_q \Phi - \dfrac{1}{J_m} R_f \omega - \dfrac{1}{J_m} \hat{\tau}_L \\ \dfrac{d^3 y_{f2}}{dt^3} = \dfrac{n_p \Phi}{J_m} \left(-\dfrac{R_s}{L} i_q - n_p \omega i_d - \dfrac{1}{L} n_p \omega \Phi \right) \\ \qquad - \dfrac{R_f}{J_m} \left(\dfrac{1}{J_m} n_p i_q \Phi - \dfrac{1}{J_m} R_f \omega - \dfrac{1}{J_m} \hat{\tau}_L \right) + \dfrac{n_p \Phi}{J_m} u_{fq} \end{cases} \tag{5}$$

Let $v_1 = \frac{dy_{f1}}{dt}$ and $v_2 = \frac{d^3 y_{f2}}{dt^3}$ be the intermediate variables, then

$$\begin{bmatrix} v_1 \\ v_2 \end{bmatrix} = \begin{bmatrix} A_1 \\ A_2 \end{bmatrix} + B \begin{bmatrix} u_{fd} \\ u_{fq} \end{bmatrix} \tag{6}$$

where

$$\begin{aligned} A_1 &= -\frac{R_s}{L} i_d + n_p \omega i_q, \\ A_2 &= \frac{n_p \Phi}{J_m} \left(-\frac{R_s}{L} i_q - n_p \omega i_d - \frac{1}{L} n_p \omega \Phi \right) \\ &\quad - \frac{R_f}{J_m} \left(\frac{1}{J_m} n_p i_q \Phi - \frac{1}{J_m} R_f \omega - \frac{1}{J_m} \hat{\tau}_L \right), \\ B_{11} &= \frac{1}{L}, \\ B_{12} &= B_{21} = 0, \\ B_{22} &= \frac{n_p \Phi}{J_m}. \end{aligned}$$

As long as matrix B is nonsingular, the system is said to be linearized [8]. By the coordinate transformation of (6), the input-output feedback linearization system can be derived as:

$$u_f = \begin{bmatrix} u_{fd} \\ u_{fq} \end{bmatrix} = B^{-1} \begin{bmatrix} v_1 - A_1 \\ v_2 - A_2 \end{bmatrix} \tag{7}$$

In order to achieve fast transient response, v_1 and v_2 are designed by the pole-placement method as follows:

$$v_1 = k_1 \left(i_d^* - i_d \right) \tag{8}$$

$$v_2 = k_2 \left(\theta^* - \theta \right) - k_3 \dot{\theta} - k_4 \ddot{\theta} \tag{9}$$

where k_1, k_2, k_3 and k_4 are the positive control parameters.

From (7), by using $i_d^* = 0$ the FBL controller is derived as:

$$\begin{cases} u_{fd} = R_s i_d - n_p L \omega i_q - L k_1 i_d \\ u_{fq} = R_s i_q + n_p L \omega i_d + n_p \omega \Phi \\ \qquad + \dfrac{R_f L}{n_p \Phi} \left(\dfrac{1}{J_m} n_p i_q \Phi - \dfrac{1}{J_m} R_f \omega - \dfrac{1}{J_m} \hat{\tau}_L \right) \\ \qquad + \dfrac{J_m L}{n_p \Phi} \left(k_2 \left(\theta^* - \theta \right) - k_3 \dot{\theta} - k_4 \ddot{\theta} \right) \end{cases} \tag{10}$$

C. DESIGN OF EPCH

The model of the Hamiltonian system with dissipation can be expressed as follows:

$$\begin{cases} \dot{x} = \left[J(x) - R(x) \right] \dfrac{\partial H(x)}{\partial x} + g(x) u_e \\ y = g^T(x) \dfrac{\partial H(x)}{\partial x} \end{cases} \tag{11}$$

where $R(x) = R^T(x) \geq 0$ is the dissipation, $J(x) = -J^T(x)$ is the interconnection structure, and $H(x)$ represents the total stored energy function of the system.

Define the state vector, input vector and output vector as:

$$x = \begin{bmatrix} x_1 & x_2 & x_3 & x_4 \end{bmatrix}^T = \begin{bmatrix} L i_d & L i_q & J_m \omega & \theta \end{bmatrix}^T \tag{12}$$

$$u_e = \begin{bmatrix} u_{ed} & u_{eq} \end{bmatrix}^T \tag{13}$$

$$y = \begin{bmatrix} i_d & i_q \end{bmatrix}^T \tag{14}$$

The Hamiltonian function of the system is given as:

$$H(x) = \frac{1}{2}\left[\frac{1}{L}{x_1}^2 + \frac{1}{L}{x_2}^2 + \frac{1}{J_m}{x_3}^2\right] + \tau_L x_4 \tag{15}$$

the model (1) can be expressed in the form of (11), with

$$\begin{aligned} J(x) &= \begin{bmatrix} 0 & 0 & 0 & n_p x_2 \\ 0 & 0 & 0 & -n_p(x_1+\Phi) \\ 0 & 0 & 0 & 1 \\ -n_p x_2 & n_p(x_1+\Phi) & -1 & 0 \end{bmatrix} \\ R(x) &= \begin{bmatrix} R_s & 0 & 0 & 0 \\ 0 & R_s & 0 & 0 \\ 0 & 0 & R_f & 0 \\ 0 & 0 & 0 & 0 \end{bmatrix} \\ g(x) &= \begin{bmatrix} 1 & 0 \\ 0 & 1 \\ 0 & 0 \\ 0 & 0 \end{bmatrix} \end{aligned} \tag{16}$$

To maintain the constant flux operation of the motor control system, i_d^* is usually set to be zero. When the controlled system reaches the required equilibrium, $\frac{d\omega}{dt} = 0$. Thus, according to (1) and (2), $i_q^* = \frac{\hat{\tau}_L + R_f\omega^*}{n_p\Phi}$ can be obtained. The desired equilibrium state for PMSM system can be selected as:

$$x^* = \begin{bmatrix} Li_d^* & Li_q^* & Li_q^* & \theta^* \end{bmatrix}^T \tag{17}$$

Let $\tilde{x} = x - x^*$ be the state error. The expected energy function $H_d(\tilde{x})$ of the closed-loop system is constructed:

$$\begin{aligned} H_d(\tilde{x}) = \frac{1}{2}\Big[\frac{1}{L}\left(x_1 - x_1^*\right)^2 + \frac{1}{L}\left(x_2 - x_2^*\right)^2 + \frac{1}{J_m}\left(x_3 - x_3^*\right)^2 \\ + \rho\left(x_4 - x_4^*\right)^2\Big] \end{aligned} \tag{18}$$

where $H_d(\tilde{x}) > 0, H_d(0) = 0$.

Assume J_a and R_a satisfying

$$\begin{aligned} J_a(x) &= \begin{bmatrix} 0 & J_{12} & J_{13} & J_{14} \\ -J_{12} & 0 & J_{23} & J_{24} \\ -J_{13} & -J_{23} & 0 & J_{34} \\ -J_{14} & -J_{24} & -J_{34} & 0 \end{bmatrix} \\ R_a &= \begin{bmatrix} r & 0 & 0 & 0 \\ 0 & r & 0 & 0 \\ 0 & 0 & 0 & 0 \\ 0 & 0 & 0 & r_m \end{bmatrix} \end{aligned} \tag{19}$$

and feedback control $u = \alpha(x)$ satisfying

$$\begin{aligned} g(x)u_e = &\left[J_a - R_a - J\left(x^*\right)\right]\frac{\partial H_d(\tilde{x})}{\partial \tilde{x}} \\ &+ \left[J(\tilde{x}) - R(x) - R\left(x^*\right)\right]\left[\frac{\partial H_d(\tilde{x})}{\partial \tilde{x}} - \frac{\partial H(x)}{\partial x}\right] \\ &+ g(x*)u^* \end{aligned} \tag{20}$$

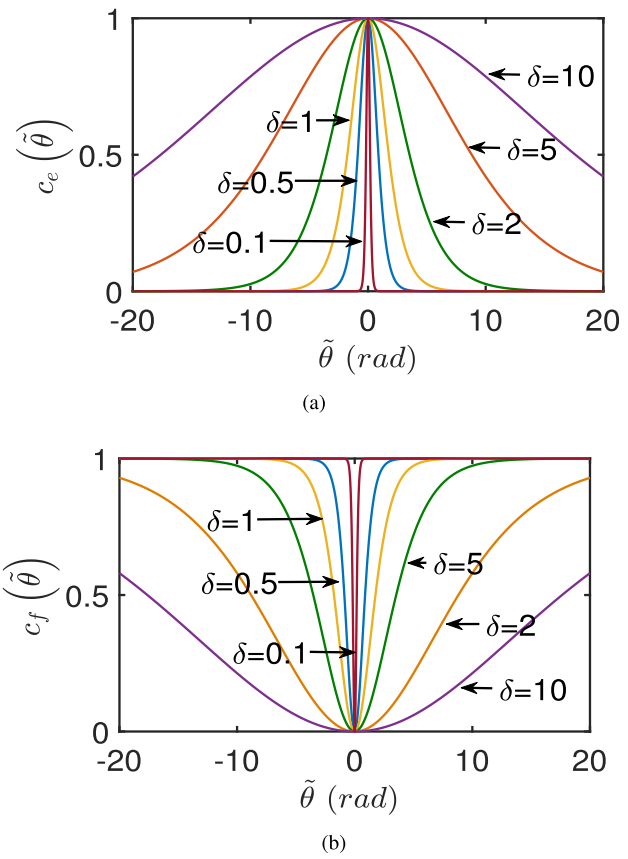

FIGURE 2. Cooperative coefficients:(a) Cooperative coefficient of EPCH controller $c_e(\tilde{\theta})$. (b) Cooperative coefficient of FBL controller $c_f(\tilde{\theta})$.

the closed-loop system can be rewritten as:

$$\dot{\tilde{x}} = \left[J_d(\tilde{x}) - R_d(\tilde{x})\right]\frac{\partial H_d(\tilde{x})}{\partial \tilde{x}} \tag{21}$$

where $J_d(\tilde{x})$ and $R_d(\tilde{x})$ are desired interconnection and damping matrix, and $J_d(\tilde{x}) = J(\tilde{x}) + J_a = -J_d^T(\tilde{x})$, $R_d(\tilde{x}) = R(\tilde{x}) + R_a = R_d^T(\tilde{x}) \geq 0$. Then, the system (21) will be asymptotically stable at $\tilde{x} = 0$ [17].

Let $J_{12} = k_0, J_{13} = -L\left(x_2 - x_2^*\right), J_{14} = -n_p\left(x_2 - x_2^*\right), J_{23} = L\left(x_1 - x_1^*\right), J_{24} = n_p\left(x_1 - x_1^*\right), J_{34} = 0$, and substituting (15)-(19) into (20), the EPCH controller is derived as:

$$\begin{cases} u_{ed} = R_s i_d^* - r\left(i_d - i_d^*\right) + k_0\left(i_q - i_q^*\right) \\ \quad - \rho L^2\left(i_q - i_q^*\right)(\theta - \theta^*) - n_p L i_q \omega \\ u_{eq} = R_s i_q^* - r\left(i_q - i_q^*\right) - k_0\left(i_d - i_d^*\right) \\ \quad + \rho L^2\left(i_d - i_d^*\right)(\theta - \theta^*) + n_p L i_d \omega + n_p \Phi \omega^* \end{cases} \tag{22}$$

where r and k_0 are adjustable parameters.

IV. DESIGN OF OPTIMIZED COOPERATIVE CONTROL

A. COOPERATIVE CONTROL STRATEGY

In order to obtain the smooth output response and avoid control signal shaking, a cooperative control strategy is designed

for the PMSM drive system. The proposed control strategy inherits the merits of FBL controller and EPCH controller, it not only implements fast dynamic tracking control, but also optimizes the input and output energy. Therefore, the cooperative control strategy is two convex combinations, that is:

$$\begin{cases} u_d = c_{fd}\left(\tilde{\theta}\right) u_{fd} + c_{ed}\left(\tilde{\theta}\right) u_{ed} \\ u_q = c_{fq}\left(\tilde{\theta}\right) u_{fq} + c_{eq}\left(\tilde{\theta}\right) u_{eq} \end{cases} \tag{23}$$

and the cooperative coefficients are selected as:

$$\begin{cases} c_{ed}\left(\tilde{\theta}\right) = c_{eq}\left(\tilde{\theta}\right) = \dfrac{4e^{-\frac{\tilde{\theta}}{\delta}}}{\left(1+e^{-\frac{\tilde{\theta}}{\delta}}\right)^2} \\ c_{fd}\left(\tilde{\theta}\right) = c_{fq}\left(\tilde{\theta}\right) = 1 - \dfrac{4e^{-\frac{\tilde{\theta}}{\delta}}}{\left(1+e^{-\frac{\tilde{\theta}}{\delta}}\right)^2} \end{cases} \tag{24}$$

where $\tilde{\theta} = \theta - \theta^*$ is the error signal between the desired and actual position, $c_{fd}\left(\tilde{\theta}\right)$ and $c_{ed}\left(\tilde{\theta}\right)$ are the d-axis cooperative coefficients of FBL controller and EPCH controller, respectively, $c_{fq}\left(\tilde{\theta}\right)$ and $c_{eq}\left(\tilde{\theta}\right)$ are q-axis cooperative coefficients of the FBL controller and EPCH controller, respectively. The cooperative coefficients are functions of position error $\tilde{\theta}$, and $c_{fd}(\tilde{\theta}) \in [0, 1)$, $c_{fq}(\tilde{\theta}) \in [0, 1)$, $c_{ed}(\tilde{\theta}) \in (0, 1]$, $c_{eq}(\tilde{\theta}) \in (0, 1]$. δ is the position scale parameter. Some design requirements, such as the rise time, settling time, percent peak overshoot and steady-state error, depend on this parameter. Thus, the control paremeter needs to be adjusted properly to get good response, as described in the next section.

Combining (10), (22) and (23), the cooperative controller can be obtained as:

$$\begin{cases} u_d = c_{ed}\left(\tilde{\theta}\right)\left[R_s i_d^* - r\left(i_d - i_d^*\right) + k_0\left(i_q - i_q^*\right)\right. \\ \quad \left. -\rho L^2\left(i_q - i_q^*\right)\left(\theta - \theta^*\right) - n_p L i_q \omega\right] \\ \quad +c_{fd}\left(\tilde{\theta}\right)\left[R_s i_d - n_p L\omega i_q + L k_1\left(i_d^* - i_d\right)\right] \\ u_q = c_{eq}\left(\tilde{\theta}\right)\left[R_s i_q^* - r\left(i_q - i_q^*\right) - k_0\left(i_d - i_d^*\right)\right. \\ \quad \left. +\rho L^2\left(i_d - i_d^*\right)\left(\theta - \theta^*\right) + n_p L i_d \omega + n_p \Phi \omega^*\right] \\ \quad +c_{fq}\left(\tilde{\theta}\right)\left[R_s i_q + n_p L\omega i_d + n_p \omega \Phi\right. \\ \quad \dfrac{R_f L}{n_p \Phi}\left(\dfrac{1}{J_m} n_p i_q \Phi - \dfrac{1}{J_m} R_f \omega - \dfrac{1}{J_m}\hat{\tau}_L\right) \\ \quad \left. +\dfrac{J_m L}{n_p \Phi}\left(k_2\left(\theta^* - \theta\right) - k_3\dot{\theta} - k_4\ddot{\theta}\right)\right] \end{cases} \tag{25}$$

The control rule developed in the combination procedure is summarized. FBL method and EPCH method are complementary, so the cooperative control strategy proposed in this article makes full use of their advantages in the corresponding range. During the operation of the motor, an improved cooperative function is used to achieve smooth switching between the two. When the position tracking error is large, FBL method is applied to control the motor, in which the fast dynamic response can be obtained. When the difference is small, EPCH method is adopted to improve steady-state precision. Therefore, the cooperative control system has good dynamic and steady-state performances in the whole operation process.

B. STABILITY ANALYSIS

In this article, a cooperative control method combining FBL and EPCH is proposed. By using a smooth switching function, when $\tilde{\theta} \to \infty$, $c\left(\tilde{\theta}\right) \to 0$, the system controlled by FBL can obtain fast dynamic response, when $\tilde{\theta} = 0$, $c\left(\tilde{\theta}\right) = 1$, the system controlled by EPCH can obtain smooth dynamic response. From the aforementioned analysis, it can be concluded that the system is stable in both cases.

When $0 < \tilde{\theta} < \infty$, the cooperative function $c\left(\tilde{\theta}\right)$ is constant between 0 and 1. Since the controller of the whole system is realized by multiplying the controller of two subsystems by the continuous cooperative function, the types of the two controllers will not change during the operation. The closed-loop control system is still stable.

C. PARAMETER OPTIMIZATION USING PSO ALGORITHM

PSO as a nature-inspired evolutionary and stochastic optimization technique, is usually applied to solve computationally hard optimization problem. During an iteration of PSO, each particle updates its velocity according to its previous experience and the experience of its neighbors. Once the velocity is updated, if it is added to the current position, the new position information is obtained. By continuously updating the velocity and position of each particle, the particle is accelerated to the best position found by it so far and the global best position obtained so far by any particle, with a random weighted acceleration at each time step. The framework for the PSO algorithm is shown in Fig. 3, where v_{t+1} is the particle's velocity at the next moment, x_t is the particle's current position, W is the inertial weight. c_1 and c_2 are acceleration coefficients, *pbest* is the particle's best position so far, *gbest* is the global best position attained.

In this work, PSO algorithm is used to regulate the cooperative scale parameter δ in the cooperative controller. First, the initial parameter δ_0 are obtained according to the engineering design method, and then the optimum parameter is calculated according to the cost function.

Due to the advantages of smaller overshoot and oscillation, ITAE (Integral Time Absolute Error) is chosen as the cost function for minimization.

$$ITAE = \int_0^T t\,|e(t)|\,dt \tag{26}$$

The optimization algorithm minimizes the cost function by changing the controller parameter.

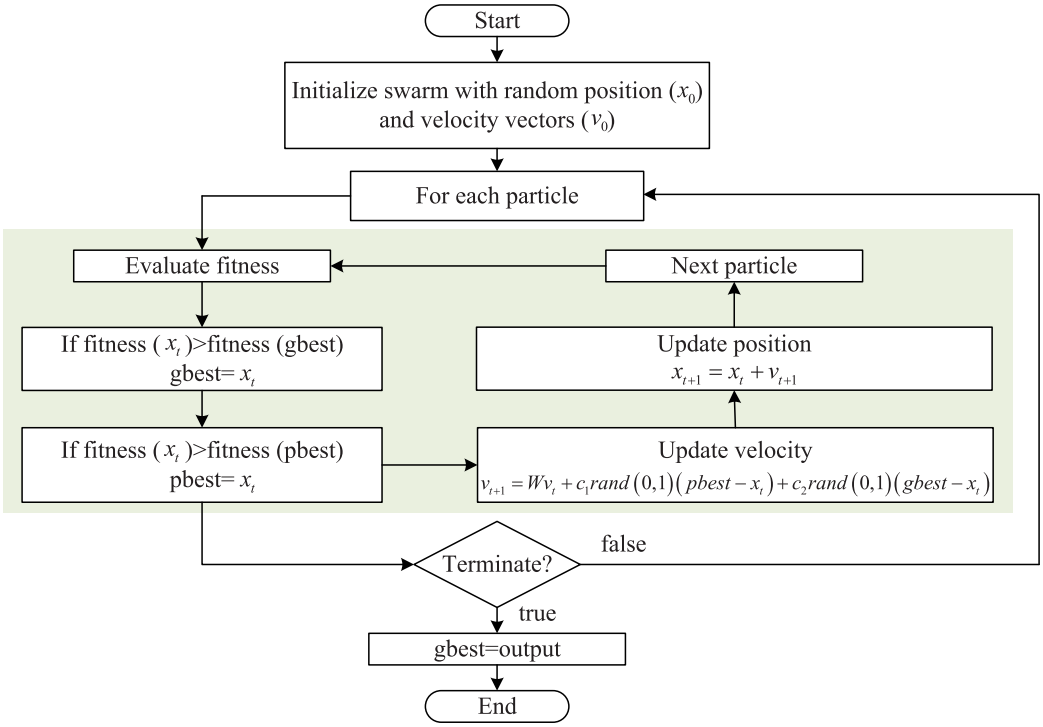

FIGURE 3. Flowchart of the PSO algorithm.

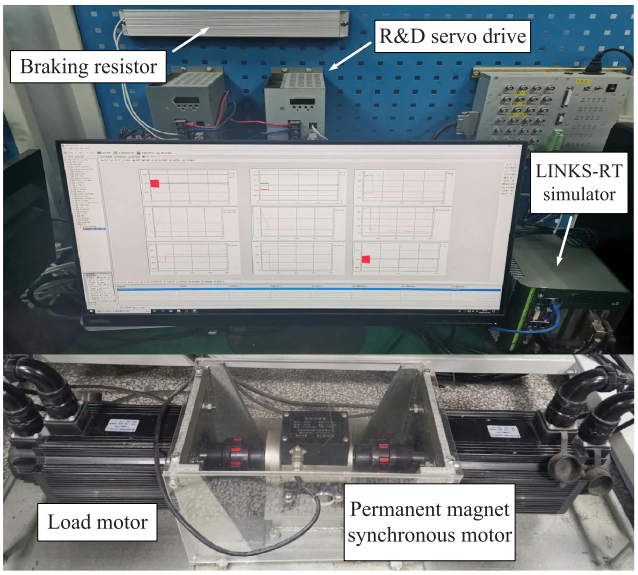

FIGURE 4. PMSM experimental platform.

TABLE 1. PMSM Parameters.

Description	Value	Unit
rated speed	1000	r/min
rated torque	10	$N \cdot m$
stator resistance	0.93	Ω
d- and q- axis inductance	3	mH
permanent magnet flux	0.32	Wb
moment of inertia	0.0027	$kg.m^2$

V. EXPERIMENTAL RESULTS

The experimental platform is shown in Fig. 4, which is completed with the LINKS-RT rapid-prototyping platform. The configuration of the experimental system is presented in Fig. 5. Both the drive and load motors are the Senstrol 130MB150A type non-salient pole PMSM. The detailed parameters of the motor are listed in Table 1. Additionally, three types of position references including exponent, step and sine are used to verify the effectiveness and superiority of the proposed cooperative method.

First, in order to test the performance of the cooperative control method under soft start, the exponential signal is used as the position reference, that is $\theta^* = 50\left(1 - e^{-2t}\right)$ rad. In Fig. 6, the actual position of the EPCH method cannot be kept close to the reference at the beginning of the operation, while the FBL shows better position tracking ability in the transient state. Further, the cooperative control method provides the more precise superposition between position quantities than the two previous control methods in both transient and states. All these remarks can be confirmed from the position errors in Fig. 7. The current responses of the three methods are shown in Fig. 8.

Then, the red curve in Fig. 9 shows the experimental results of the cooperative method under step signal, which verifies that the cooperative control method can effectively follow the position reference. The comparison of trajectory tracking capabilities of different methods is shown in Fig. 9. Due to the fast dynamic response, as for the FBL, the steady-state

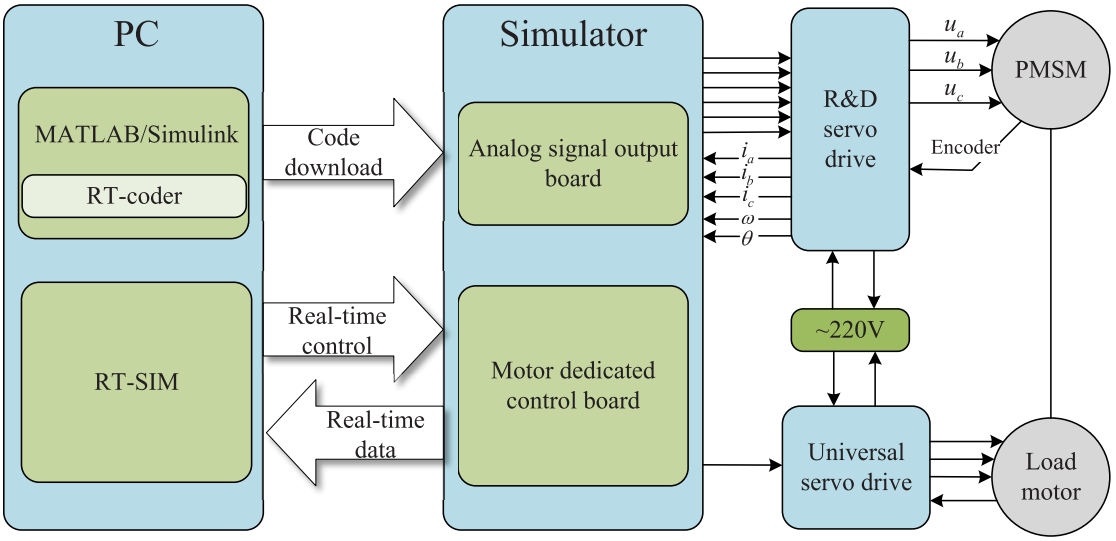

FIGURE 5. Experimental configuration of PMSM system.

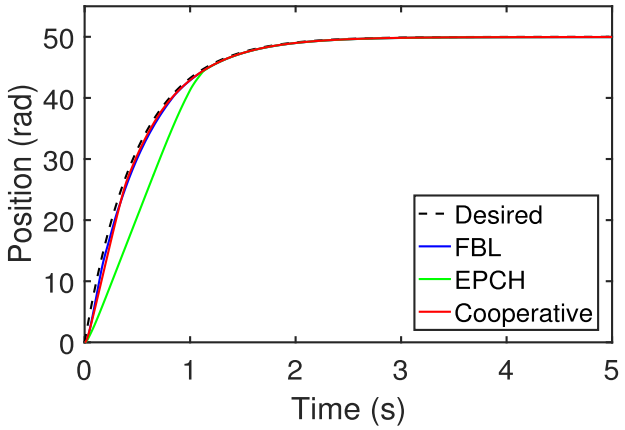

FIGURE 6. Position tracking response when $\theta^* = 50\left(1 - e^{-2t}\right)$.

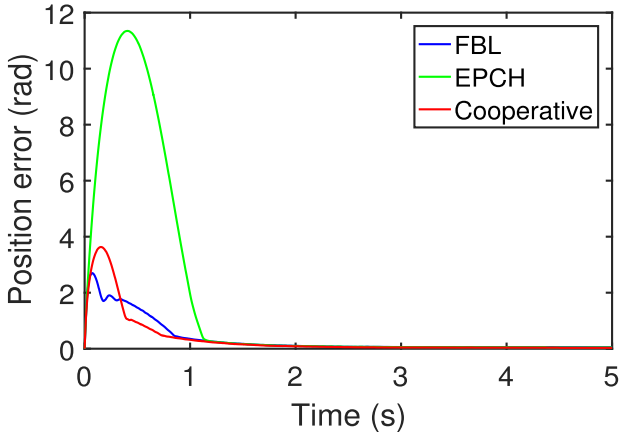

FIGURE 7. Position tracking error.

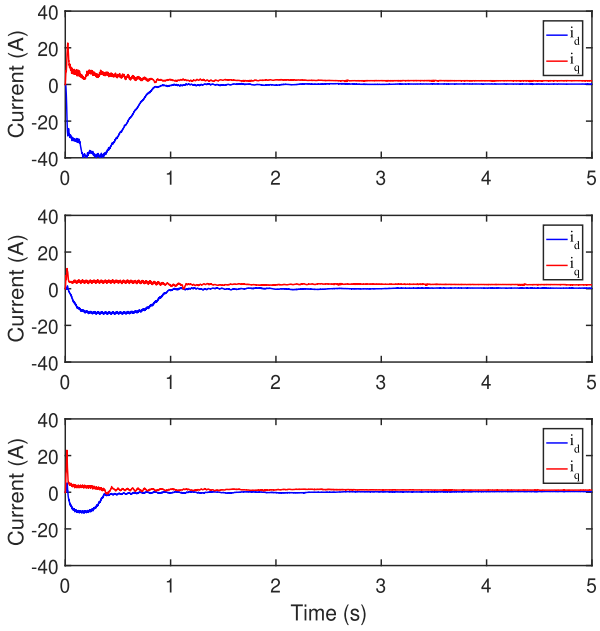

FIGURE 8. Current response.

error increases to 0.1 rad, and the overshoot even occurs. Although the steady-state error of EPCH method is reduced to 0.01 rad, the dynamic response time increases by 0.6 s. As for the traditional individual method, although the control system can track the position reference and want to obtain a satisfactory response, the contradiction between dynamic rapidity and steady-state accuracy limits their development. In contrast, because the cooperative method combines the advantages of the two and improves further, both the position tracking error and dynamic response time are significantly reduced. According to the enlarged figure, the dynamic response time of the cooperative method is 0.67 s, and the steady-state error is consistent with the EPCH method, which

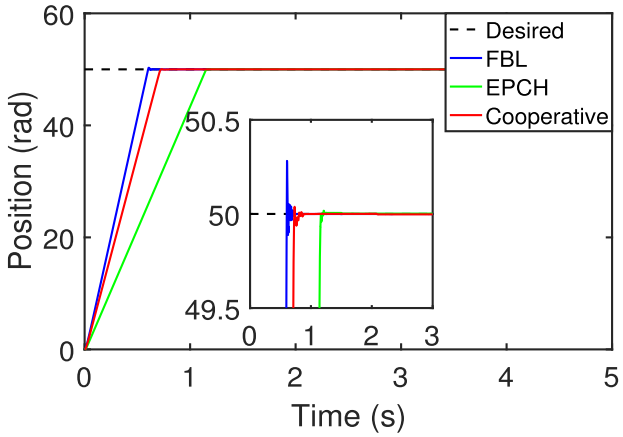

FIGURE 9. Position tracking response when $\theta^* = 50$.

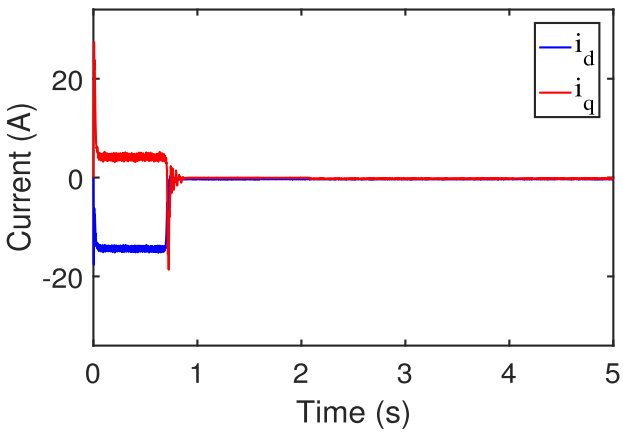

FIGURE 10. Current response.

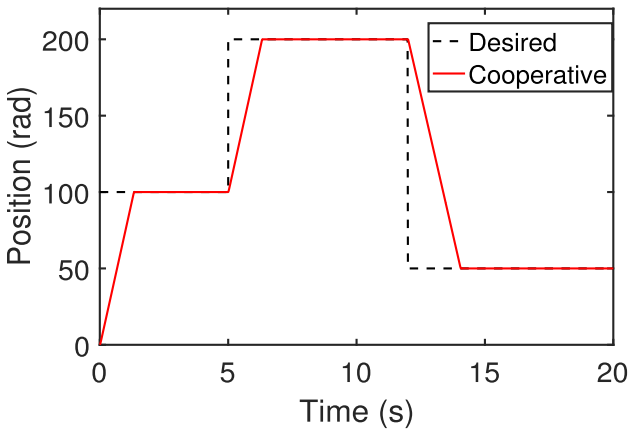

FIGURE 11. Response at different positions.

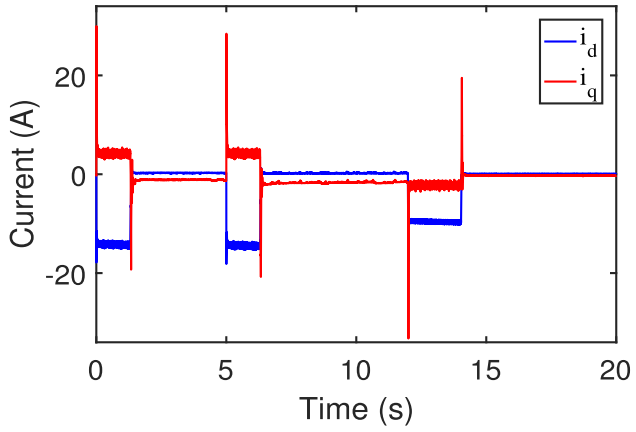

FIGURE 12. Current response.

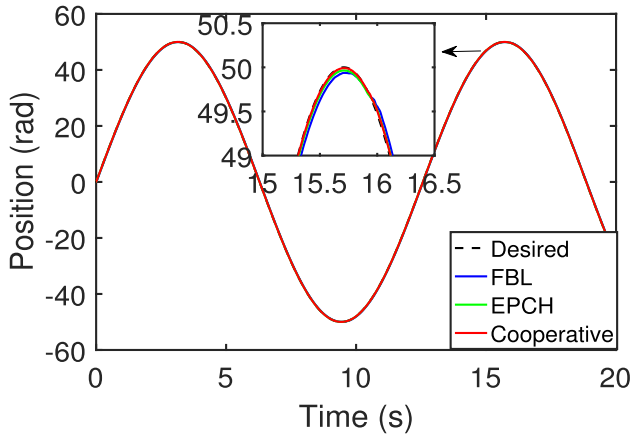

FIGURE 13. Position tracking response when $\theta^* = 50\sin(t)$.

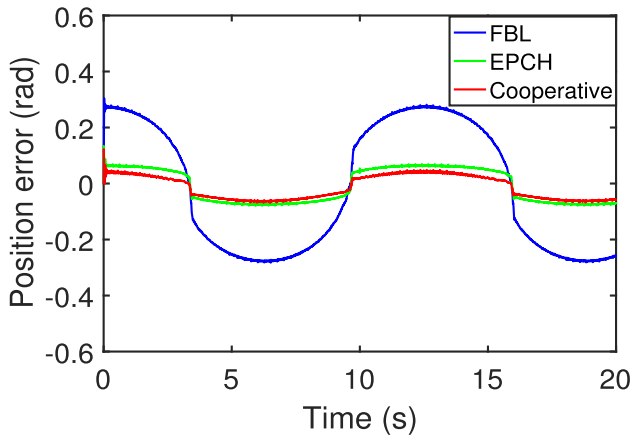

FIGURE 14. Position tracking error.

means that the motor drive can reach the reference value faster and realize high-precision operation. Overall, the key factor that makes difference between the individual method and cooperative method is the smooth switching structure based on position error in the cooperative control system. Additionally, the cooperative method has smaller current fluctuation, as shown in Fig. 10.

In order to further verify the position tracking ability of the proposed method, the experimental result at different positions is recorded. The response waveform shown in Fig. 11 gives that the proposed method still performs

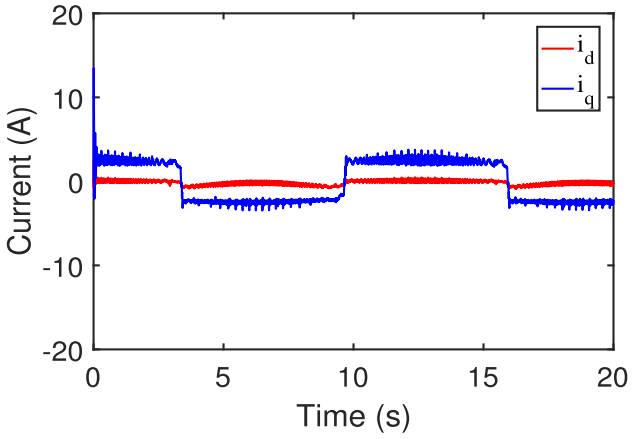

FIGURE 15. Current response.

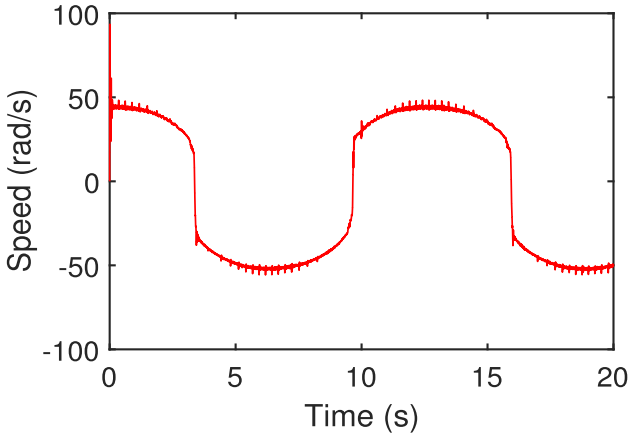

FIGURE 16. Speed tracking response.

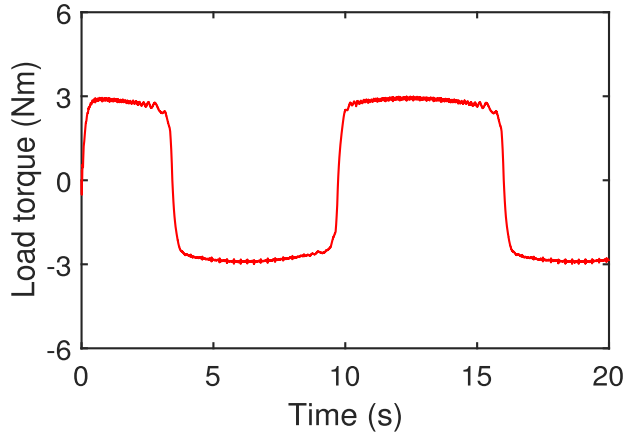

FIGURE 17. Estimated load torque.

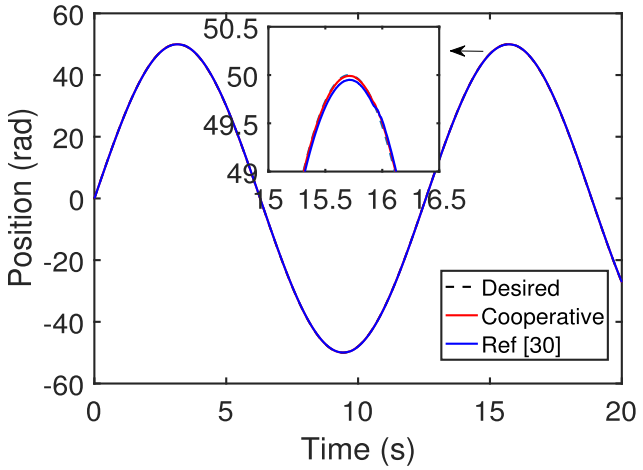

FIGURE 18. Position tracking response.

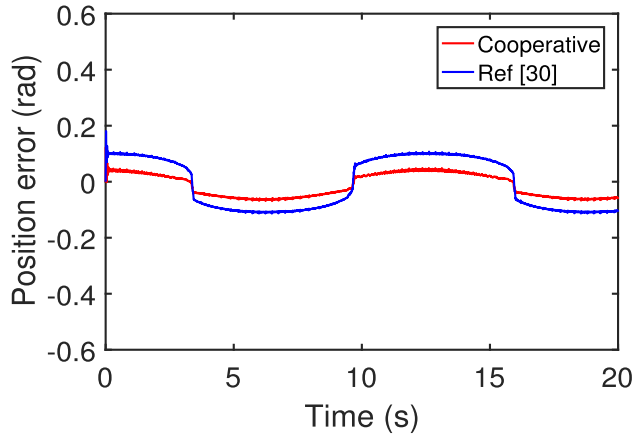

FIGURE 19. Position tracking error.

good performance. Fig. 12 shows the current response in this situation.

Fig. 13 shows the experimental results of position tracking with different methods. A sinusoidal signal is used as the position reference in this part. The results indicate that the position fluctuations of the three methods are basically the same. The detailed waveform of position tracking error is shown in Fig. 14. The experimental results show that the maximum position errors of FBL method and EPCH method are 0.3 rad and 0.05 rad, respectively. Both of them are greater than 0.016 rad of the cooperative method. Therefore, the cooperative method has a better position tracking performance. In addition, when a constant 3 Nm load is added, the performance of the proposed method can still remain smoother and vibration-less. The waveforms of speed, current and load estimation for the cooperative method are shown in Fig. 15-17.

Finally, the comparison between position tracking results of the proposed method and [30] is shown in Fig. 18. Both methods can make the system work stably under sinusoidal signal, but the proposed method has better position tracking capability. For example, in Fig. 19, the position error of [30] is 0.1 rad, but that of the proposed method is successfully reduced by 84%. Because the deadbeat controller in [30] can only accelerate the current loop, the dynamic response speed of the whole closed-loop system is limited. On the other hand, owing to the introduction of the PSO algorithm to select

the appropriate cooperative parameter, the proposed method performs better both in dynamic and steady states.

VI. CONCLUSION

Faced with the challenge of realizing the dual objectives of fast dynamic response and high steady-state precision, a cooperative control strategy is proposed for PMSM drives in this article. Different from the traditional hybrid control with the cascade control structure, the proposed cooperative control strategy is based on the convex combination, in which the control mode is switched between FBL and EPCH according to the real-time position error. In this method, fast dynamic response can be provided by using FBL, and EPCH is applied to ensure high steady-state precision. By this means, good dynamic and steady-state performances can be achieved. Meanwhile, to account for the parameter adjustment in practice, PSO algorithm is introduced to select the appropriate control gains.

The comparison experiments are presented to illustrate that the proposed method overcomes the limitations of FBL and EPCH in improving the control performance of PMSM, and shows a satisfying performance with good dynamic response and high steady-state precision. In addition, compared with the cooperative control proposed in [30], the superiority of the proposed method to indeed guarantee and further improve the control performance are fully verified.

On the other hand, the PSO algorithm has the advantages of simplicity and easy-implemented. Perhaps more optimization algorithms could be considered for a general discussion and research in the future work.

REFERENCES

[1] F. Wang, K. Zuo, P. Tao, and J. Rodriguez, "High performance model predictive control for PMSM by using stator current mathematical model self-regulation technique," *IEEE Trans. Power Electron.*, vol. 35, no. 12, pp. 13652–13662, Dec. 2020.

[2] B. Zhang and X. Tang, "High-performance state feedback controller for permanent magnet synchronous motor," *ISA Trans.*, Feb. 2021, doi: 10.1016/j.isatra.2021.02.009.

[3] X. Sun, H. Yu, J. Yu, and X. Liu, "Design and implementation of a novel adaptive backstepping control scheme for a PMSM with unknown load torque," *IET Electr. Power Appl.*, vol. 13, no. 4, pp. 445–455, 2019.

[4] T. Yuan, D. Wang, X. Wang, X. Wang, and Z. Sun, "High-precision servo control of industrial robot driven by PMSM-DTC utilizing composite active vectors," *IEEE Access*, vol. 7, pp. 7577–7587, 2019.

[5] J. Long, M. Yang, Y. Chen, K. Liu, and D. Xu, "Current-controller-free self-commissioning scheme for deadbeat predictive control in parametric uncertain SPMSM," *IEEE Access*, vol. 9, pp. 289–302, 2021.

[6] N. Amiri, V. Fakhari, and S. Sepahvand, "Motion control of a caterpillar robot using optimized feedback linearization and sliding mode controllers," *Int. J. Dyn. Control*, vol. 9, no. 3, pp. 1107–1116, Sep. 2021.

[7] A. Ammar, A. Kheldoun, B. Metidji, T. Ameid, and Y. Azzoug, "Feedback linearization based sensorless direct torque control using stator flux MRAS-sliding mode observer for induction motor drive," *ISA Trans.*, vol. 98, pp. 382–392, Mar. 2020.

[8] X. Liu, H. Yu, J. Yu, and L. Zhao, "Combined speed and current terminal sliding mode control with nonlinear disturbance observer for PMSM drive," *IEEE Access*, vol. 6, pp. 29594–29601, 2018.

[9] X. Meng, H. Yu, J. Zhang, T. Xu, H. Wu, and K. Yan, "Disturbance observer-based feedback linearization control for a quadruple-tank liquid level system," *ISA Trans.*, Apr. 2021, doi: 10.1016/j.isatra.2021.04.021.

[10] T. Tarczewski and L. M. Grzesiak, "Constrained state feedback speed control of PMSM based on model predictive approach," *IEEE Trans. Ind. Electron.*, vol. 63, no. 6, pp. 3867–3875, Jun. 2016.

[11] X. Sun, C. Hu, G. Lei, Y. Guo, and J. Zhu, "State feedback control for a PM hub motor based on gray wolf optimization algorithm," *IEEE Trans. Power Electron.*, vol. 35, no. 1, pp. 1136–1146, Jan. 2020.

[12] X. Sun, Z. Jin, Y. Cai, Z. Yang, and L. Chen, "Grey wolf optimization algorithm based state feedback control for a bearingless permanent magnet synchronous machine," *IEEE Trans. Power Electron.*, vol. 35, no. 12, pp. 13631–13640, Dec. 2020.

[13] T. Zhao and G. Duan, "Interconnection structure preservation design for a type of port-controlled Hamiltonian systems—A parametric approach," *IET Control Theory Appl.*, vol. 15, no. 3, pp. 338–347, Feb. 2021.

[14] A. Moreschini, M. Mattioni, S. Monaco, and D. Normand-Cyrot, "Stabilization of discrete port-Hamiltonian dynamics via interconnection and damping assignment," *IEEE Control Syst. Lett.*, vol. 5, no. 1, pp. 103–108, Jan. 2021.

[15] J. Yu, W. Pei, and C. Zhang, "A loss-minimization port-controlled Hamilton scheme of induction motor for electric vehicles," *IEEE/ASME Trans. Mechatronics*, vol. 20, no. 6, pp. 2645–2653, Dec. 2015.

[16] B. Fu, S. Li, X. Wang, and L. Guo, "Output feedback based simultaneous stabilization of two port-controlled Hamiltonian systems with disturbances," *J. Franklin Inst.*, vol. 356, no. 15, pp. 8154–8166, Oct. 2019.

[17] H. Yu, J. Yu, J. Liu, and Q. Song, "Nonlinear control of induction motors based on state error PCH and energy-shaping principle," *Nonlinear Dyn.*, vol. 72, nos. 1–2, pp. 49–59, 2013.

[18] F. Aghili, "Optimal feedback linearization control of interior PM synchronous motors subject to time-varying operation conditions minimizing power loss," *IEEE Trans. Ind. Electron.*, vol. 65, no. 7, pp. 5414–5421, Jul. 2018.

[19] A. Campos-Rodríguez, J. P. García-Sandoval, V. González-Álvarez, and A. González-Álvarez, "Hybrid cascade control for a class of nonlinear dynamical systems," *J. Process Control*, vol. 76, pp. 141–154, Apr. 2019.

[20] Z. Song, H. Park, F. P. Delgado, H. Wang, Z. Li, H. F. Hofmann, J. Sun, and J. Hou, "Simultaneous identification and control for hybrid energy storage system using model predictive control and active signal injection," *IEEE Trans. Ind. Electron.*, vol. 67, no. 11, pp. 9768–9778, Nov. 2020.

[21] Y. Jiang, W. Xu, C. Mu, and Y. Liu, "Improved deadbeat predictive current control combined sliding mode strategy for PMSM drive system," *IEEE Trans. Veh. Technol.*, vol. 67, no. 1, pp. 251–263, Jan. 2018.

[22] W. Ding, G. Liu, and P. Li, "A hybrid control strategy of hybrid-excitation switched reluctance motor for torque ripple reduction and constant power extension," *IEEE Trans. Ind. Electron.*, vol. 67, no. 1, pp. 38–48, Jan. 2020.

[23] M. J. Mahmoodabadi and T. Soleymani, "Optimum fuzzy combination of robust decoupled sliding mode and adaptive feedback linearization controllers for uncertain under-actuated nonlinear systems," *Chin. J. Phys.*, vol. 64, pp. 241–250, Apr. 2020.

[24] Y. Wang, H. Yu, H. Wu, and X. Liu, "Trajectory tracking of flexible-joint robots actuated by PMSM via a novel smooth switching control strategy," *Appl. Sci.*, vol. 9, no. 20, pp. 4382–4397, 2019.

[25] K. Lee, H. Kim, J. Yoon, H.-S. Oh, J.-H. Park, B.-H. Park, H. Park, and Y. Lee, "An asynchronous boost converter with time-based dual-mode control for wide load range and high efficiency in SSD applications," *IEEE Trans. Ind. Electron.*, vol. 67, no. 12, pp. 10520–10530, Dec. 2020.

[26] L. Lyu, Z. Chen, and B. Yao, "Development of parallel-connected pump-valve-coordinated control unit with improved performance and efficiency," *Mechatronics*, vol. 70, pp. 1–10, Oct. 2020.

[27] X. Wang, Z. Wang, Z. Xu, M. Cheng, and Y. Hu, "Optimization of torque tracking performance for direct-torque-controlled PMSM drives with composite torque regulator," *IEEE Trans. Ind. Electron.*, vol. 67, no. 12, pp. 10095–10108, Dec. 2020.

[28] Z. Hao, Y. Yang, Y. Gong, Z. Hao, C. Zhang, H. Song, and J. Zhang, "Linear/nonlinear active disturbance rejection switching control for permanent magnet synchronous motors," *IEEE Trans. Power Electron.*, vol. 36, no. 8, pp. 9334–9347, Aug. 2021.

[29] C. Elmas and O. Ustun, "A hybrid controller for the speed control of a permanent magnet synchronous motor drive," *Control Eng. Pract.*, vol. 16, no. 3, pp. 260–270, Mar. 2008.

[30] Y. Zhao and H. Yu, "Cooperative control of deadbeat predictive and state error port-controlled Hamiltonian method for permanent magnet synchronous motor drives," *IET Electr. Power Appl.*, vol. 15, no. 10, pp. 1343–1357, Oct. 2021, doi: 10.1049/elp2.12104.
[31] C. Miao, G. Chen, C. Yan, and Y. Wu, "Path planning optimization of indoor mobile robot based on adaptive ant colony algorithm," *Comput. Ind. Eng.*, vol. 156, no. 3, pp. 1–10, Jun. 2021.
[32] M. J. Mahmoodabadi, S. Momennejad, and A. Bagheri, "Online optimal decoupled sliding mode control based on moving least squares and particle swarm optimization," *Inf. Sci.*, vol. 268, pp. 342–356, Jun. 2014.
[33] B. Deboon, S. Nokleby, and C. Rossa, "Multi-objective gain optimizer for a multi-input active disturbance rejection controller: Application to series elastic actuators," *Control Eng. Pract.*, vol. 109, pp. 104733–104746, Apr. 2021.
[34] J. Yan, H. Kong, and Z. Man, "An improved Hopfield Lagrange network with application on motor efficiency optimization," *Asian J. Control*, Feb. 2021, doi: 10.1002/asjc.2507.

YUJIAO ZHAO received the B.S. degree in engineering from Qufu Normal University at Rizhao, Rizhao, China, in 2019. She is currently pursuing the M.S. degree in control science and engineering with Qingdao University. Her research interests include the power electronics, motor drive, and electrical energy conversion.

HAISHENG YU received the B.S. degree in electrical automation from the Harbin University of Civil Engineering and Architecture, in 1985, the M.S. degree in computer applications from Tsinghua University, in 1988, and the Ph.D. degree in control science and engineering from Shandong University, China, in 2006. He is currently a Professor with the School of Automation, Qingdao University, China. His research interests include electrical energy conversion and motor control, applied nonlinear control, computer control, and intelligent systems.

SHIXIAN WANG received the B.S. degree in engineering from Qufu Normal University at Rizhao, Rizhao, China, in 2019. He is currently pursuing the M.S. degree in control science and engineering with Shandong University at Weihai. His research interests include the pattern recognition, deep learning, and bioinformatics.